



# Dynamic Strain Sensors and Accelerometers for Structural Testing

**Cases of Measurements on a Civil Structure  
and on the GVT of an F-16 Aircraft**

Written By  
Carmine Salzano, PCB Piezotronics Inc.

# Dynamic Strain Sensors and Accelerometers for Structural Testing: Cases of Measurements on a Civil Structure and on the GVT of an F-16 Aircraft

C. Salzano<sup>1</sup>

<sup>1</sup> PCB Piezotronics Inc., Depew, USA. csalzano@pcb.com

**Abstract.** Ground vibration testing (GVT) of aircraft is a measurement campaign performed in the development process of an aircraft, with the objective of obtaining experimental data on the aircraft to validate and update the structural dynamic models, which can, in turn, be used to predict important behavior, such as flutter. These measurements are usually carried out using standard accelerometers, and are used to identify the displacement mode shapes. However, the use of strain sensors in vibration and modal related applications has recently gained popularity, due to some advantages, such as sensor size and the fact that strain relates directly to stress.

The quartz strain sensor has very unique features: it is reusable, making it very cost effective, and it is easy to mount with cyanoacrylate, just like an accelerometer. And just like an accelerometer, it can be used with a direct connection to the measurement system thanks to ICP® technology. Furthermore, this type of sensor is available in different versions offering wide frequency range, high sensitivity, and high resolution.

In this paper, the main results of a GVT campaign on an F-16 aircraft will be shown, where the full aircraft was instrumented with accelerometers, and one of the wings was also fully instrumented with piezo strain sensors. The main results of the test campaign will be shown, where both strain sensor and accelerometer measurements are processed simultaneously, resulting in the strain and displacement mode shapes, respectively. Some characteristics and advantages of carrying out the tests this way will also be presented.

**Keywords:** Strain Sensors, Strain Modal Analysis, Ground Vibration Testing

## 1 Introduction

Structural testing refers to specific dynamic tests on any given structure, small or large. These dynamic tests involve a test and measurement system composed of various types of sensors and a suitable acquisition system with related analysis software. We can divide these tests according to the purpose, but overall, we categorize them into two types according to measurement setup: modal analysis and operational modal analysis (OMA). Modal analysis involves the excitation of the structure with essentially two types of transducer technologies, while for operational modal analysis (OMA), external excitation is not required as the motion of the dynamic structure itself is analyzed during its normal operating conditions. In any case, the response of the system is detected by sensors that may utilize the same technology in both types of tests.

In this paper, the sensor technologies used for detecting the structural response during both OMA and modal analysis will be described, with particular attention to strain sensors, which can be a useful addition to the sensors traditionally used for such tests. The second part of the paper will describe an application of strain sensors for a civil structure test and ground vibration testing (GVT) on an aircraft as practical use cases for such sensor technologies [1].

The GVT of aircraft is often considered a very important step in aircraft design, being most useful in identifying the structural dynamics of the aircraft [2, 3], which in turn are used to correlate and update numerical models. This sort of testing has evolved from lengthy tests, such as normal mode testing, to more efficient (but still accurate) methodologies using broadband excitation signals and controlled multiple-input multiple-output (MIMO) excitation methods [4]. Nonetheless, various types of improvements are still being sought by the aircraft industry, both in reducing testing time and in enhancing quality and interpretation of the data, that is, to obtain more relevant results from the same test.

One way to achieve this is to use different types of sensors that can yield information that could not be obtained before. In this sense, even though modal testing has long been associated with the use of accelerometers, the use of strain sensors in modal analysis [5, 6] has gained increased interest from both industry and academia [7, 8, 9].

Another application of dynamic strain measurements is related to the strain-displacement relations [10], or more specifically to load prediction using strain measurements.

## 2 Sensors for Structural Test Setup

The setup of a structural analysis test system involves sensor technologies for both excitation and response measurement, as mentioned. Focusing specifically on OMA, the piezoelectric accelerometer, typically ICP® (also known as IEPE), is the most commonly used technology for measuring structural response.

Various technologies are available for exciting the structure during testing. For modal analysis, excitation involves the use of a piezoelectric force transducer, with the same sensor piezoelectric (ICP) technology for measuring the response of the structure following excitation. The piezoelectric force sensor shown in Figure 1 uses a piezoelectric crystal, typically quartz, as its sensing element [11].

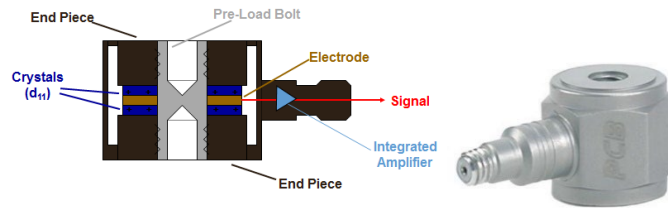


Figure 1: Piezoelectric force sensor schematic and photo

Quartz force sensors are recommended for dynamic force applications. They are not used as 'load cells' for static applications. Measurements of dynamic oscillating forces, impacts, or high-speed compression/tension under varying conditions may require sensors with special capabilities. Fast response, ruggedness, stiffness comparable to solid steel, extended ranges, and the ability to also measure quasi-static forces are standard features associated with quartz force sensors. When force is applied to this sensor, the quartz crystals generate an electrostatic charge proportional to the input force. This output is collected on the electrodes sandwiched between the crystals and is then either routed directly to an external charge amplifier or converted to a low impedance voltage signal within the sensor.

ICP force sensors incorporate a built-in MOSFET microelectronic amplifier to convert the high impedance charge output into a low impedance voltage signal for recording. ICP sensors, powered from a separate constant current source, operate over long ordinary coaxial or ribbon cable without signal degradation. The low impedance voltage signal is not affected by triboelectric cable noise or contaminants. In addition to ease of operation, ICP force sensors offer significant advantages over charge mode types. Because of the low impedance output and solid-state, hermetic construction, ICP force sensors are well suited for continuous, unattended force monitoring in harsh factory environments. Also, the ICP sensor's cost-per-channel is substantially lower, since they operate through standard, low-cost coaxial cable, and do not require expensive charge amplifiers.

The force sensor used for suitable excitation of the structure under test can be found in two types of devices: specialized impact hammers, or electrodynamic shakers. The impact hammer has a force sensor at its tip, similar in principle and operation to the one just described. The electrodynamic shaker, on the other hand, uses a stinger to excite the force sensor exactly as described above.

## 3 Accelerometers for Structural Testing

The most widely used sensor for measuring the response in a structural dynamic test is undoubtedly the accelerometer. The accelerometer technologies used in dynamic tests can be divided into piezoelectric or MEMS types. Piezoelectric accelerometers were originally created with charging output, but then the technology of amplified piezoelectric accelerometers, better known as IEPE or ICP, was developed. In contrast, MEMS are mainly of two types: piezoresistive, used for tests at high acceleration values such as impacts and shocks; and capacitive, which can sometimes also be used in these types of dynamic measurements characterized by limited acceleration values. The main benefit of MEMS capacitive compared to ICP lies in the possibility of measuring from 0Hz. This is not

essential for a dynamic test, which is why the ICP accelerometer has established itself as the main sensor for the structural response both for modal analysis and for OMA.

An ICP accelerometer is a sensor that generates an electrical output proportional to applied acceleration. ICP accelerometers are designed to measure vibration and shock for a wide variety of applications. They are simple to use and accurate over a wide frequency range, making them the recommended choice for many testing situations.

An accelerometer structure can be characterized as a single degree of freedom system that is governed by Newton's Law of Motion,  $F=MA$ .

A variety of mechanical designs are used to perform the transduction required for ICP accelerometers. The designs consist of sensing crystals that are attached to a seismic mass. A preload ring or stud applies a force to the sensing element assembly to make a rigid structure and insure linear behavior. Under acceleration, the seismic mass causes stress on the sensing crystals, which results in a proportional electrical output. The output is collected on electrodes and transmitted by wires connected to the microelectronic circuitry in ICP accelerometers. The schematic of the ICP accelerometer is shown in Figure 2 below.

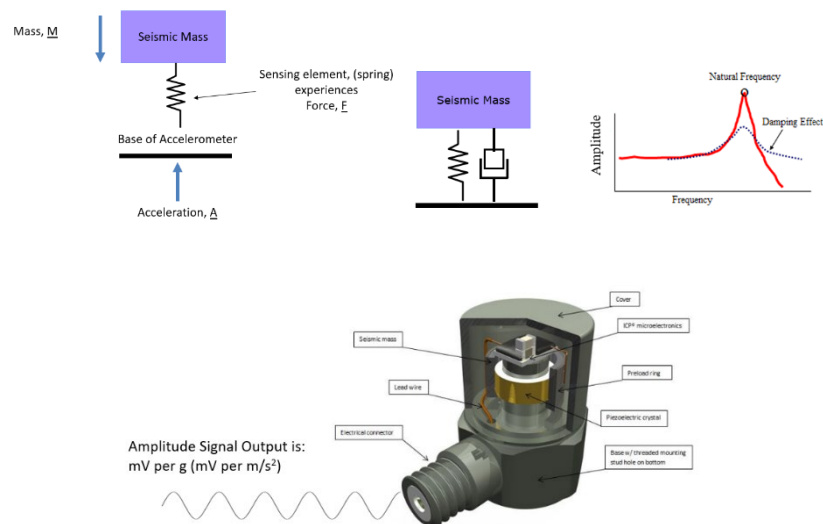


Figure 2: ICP® (IEPE) operating principle and schematic of an accelerometer

There are many types of ICP accelerometers depending on specific testing requirements, but for now we will only briefly describe the main characteristics required for an accelerometer used for structural testing.

Desirable specifications for structural test accelerometers are: lightweight, high sensitivity, low frequency response, good phase characteristics, low base strain sensitivity, no problems driving long cables (ICP), single axis or triaxial, TEDS transducer electronic data sheet (easy setup of large tests), miniature, cubic (for easy alignment), adhesive (and mounting) base, low cost (as there are oftentimes tens to hundreds of channels in a test), frequency range (5%) from close to 0Hz to ~3kHz, and sensitivity from 100mV/g to 1V/g. In Figure 3, some examples of modal or operational modal test accelerometers are shown.

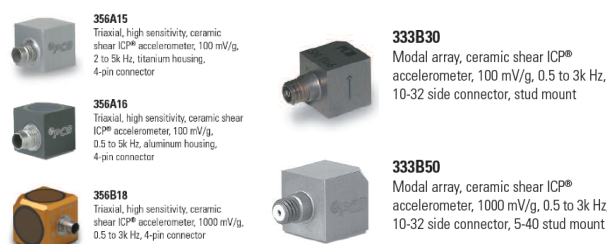


Figure 3: ICP® (IEPE) accelerometers for structural test

## 4 Strain Modal Analysis

The use of strain sensors in modal analysis follows the typical modal formulation, which is similar to the classical modal analysis form, but with some differences. The modal superposition can be applied to strain modal analysis, and it leads to the following formulation:

$$\varepsilon(t, p) = \sum_{r=1}^n \psi_r(p) q_r(t) \quad (1)$$

where  $\Psi_r$  is the  $r^{\text{th}}$  strain mode at point  $p$ ,  $q_r(t)$  the generalized modal coordinate and  $\varepsilon(t, p)$  is the strain at time  $t$  and at point  $p$ .

Given the theory of elasticity, the strain in a general direction is equal to the gradient of the vector component in that same direction. That is, for the displacement in the general direction  $u$ , the strain will be:

$$\varepsilon(t, p) = \nabla u(t, p) \quad (2)$$

with  $\varepsilon(t, p)$  being the strain at time  $t$  and at point  $p$ , and  $\nabla$  being the linear spatial differential operator.

The relation between a force input and a strain output, in terms of displacement and strain modes is then represented as:

$$\varepsilon = \sum_{r=1}^n \psi_r \Lambda_r^{-1} \phi_r F \quad (3)$$

where  $F$  is the time dependent force vector. Finally, the strain frequency response function (SFRF) can be obtained, in matrix form:

$$\mathbf{H}^\varepsilon = \sum_{r=1}^n \Lambda_r^{-1} \{\psi_r\} \{\phi_r\} = [\psi_r] [\Lambda_r]^{-1} [\phi_r]^T \quad (4)$$

The expansion of (4) is:

$$\begin{bmatrix} H_{11}^\varepsilon & H_{12}^\varepsilon & \cdots & H_{1N_q}^\varepsilon \\ H_{21}^\varepsilon & H_{22}^\varepsilon & \cdots & H_{2N_q}^\varepsilon \\ \vdots & \vdots & \vdots & \vdots \\ H_{N_p 1}^\varepsilon & H_{N_p 2}^\varepsilon & \cdots & H_{N_p N_q}^\varepsilon \end{bmatrix} = \sum_{r=1}^n \Lambda_r^{-1} \cdot \begin{bmatrix} \psi_{1r} \phi_{1r} & \psi_{1r} \phi_{2r} & \cdots & \psi_{1r} \phi_{N_q r} \\ \psi_{2r} \phi_{1r} & \psi_{2r} \phi_{2r} & \cdots & \psi_{2r} \phi_{N_q r} \\ \vdots & \vdots & \vdots & \vdots \\ \psi_{N_p r} \phi_{1r} & \psi_{N_p r} \phi_{2r} & \cdots & \psi_{N_p r} \phi_{N_q r} \end{bmatrix}_{N_p \times N_q} \quad (5)$$

where  $N_p$  represents the number of strain gauge measurement stations (or the number of output measurements) and  $N_q$  represents the number of excitation points (or the number of inputs).

Strain modal analysis and the use of strain gauges in modal testing can be referred to as a means of using solely strain gauges as the output sensors in modal analysis. However, there can be many benefits to combining strain gauge and accelerometer measurements [12]. On one hand, strain modes can be very hard to interpret, since by themselves they do not directly show how the structure is being displaced. If the structure being analyzed is very complicated in shape and structure (as is the case with an aircraft), then the task of interpreting the strain mode shapes becomes very complex [13]. On the other hand, the strain modes can provide valuable information that otherwise is not available by solely using accelerometers [13, 14].

Being able to visualize where strain (and therefore stress) occurs, as well as identify how the vibration modes contribute to this effect, is very valuable. Therefore, by combining strain gauge and accelerometer measurements, one can combine the ease of interpretation that comes from displacement mode shapes with the additional strain concentration information provided by the strain modes.

For mixed strain and displacement modal analysis, the modal superposition formulation has the same format, but it is composed of the displacement and strain parts [16, 17].

## 5 Piezo Strain Sensors

To carry out dynamic strain measurements, many types of sensors can be used, each one with their advantages and drawbacks. For the strain measurements in the GVT measurement campaign, piezo strain sensors were chosen (PCB 740B02). This type of reusable sensor, suitable for dynamic measurements, is structured with a quartz sensing element and microelectronics circuitry. It can only be used to measure unidirectional strain and has a grid length of 15mm.



Figure 4: ICP® (IEPE) dynamic reusable strain sensor for structural test

The advantage of this type of sensor over resistive strain gauges comes from its better signal-to-noise-ratio, due to the piezoelectric sensing element. It employs the commonly used ICP amplifier, a real charge amplifier which converts the original signal (electric charge) of the quartz into voltage proportional to the measured strain, with a nominal sensitivity of around  $50\text{mV}/\mu\epsilon$ , and a frequency range similar to that of piezo accelerometers, varying from 0.5 Hz to 100KHz (not usable to measure static loads). The sensing element of each sensor is protected by a titanium housing that is hermetically sealed, and its stiffness does not allow the use of the sensor on curved surfaces.

These sensors, unlike resistive strain gauges, can be mounted using a quick bonding cyanoacrylate gel, which makes the bonding procedure much faster and more compatible with the instrumentation timings and efforts required for a GVT test campaign. Nonetheless, proper mounting is critical to good sensor performance; as with traditional strain gauges, all surfaces must be clean, dry, and free of oils before applying the adhesive. However, the sensor can be reused and re-applied in case it is necessary. The calibration of these sensors is not done on-site, but is instead carried out in a controlled environment, where the sensors are dynamically calibrated using a steel cantilever beam.

The 740A02 strain sensor combines a quartz sensing element and microelectronic signal conditioning within a titanium housing of outer dimensions  $0.2 \times 0.6 \times 0.07$  inches [ $5,1 \times 15,2 \times 1,8$  mm]. The sensor measures in-plane normal strain along the length of the sensor (Figure 5). The sensor is designed for minimum sensitivity to transverse strain. Because the sensing element is quartz, it is inherently insensitive to pyroelectric (thermal) disturbances.

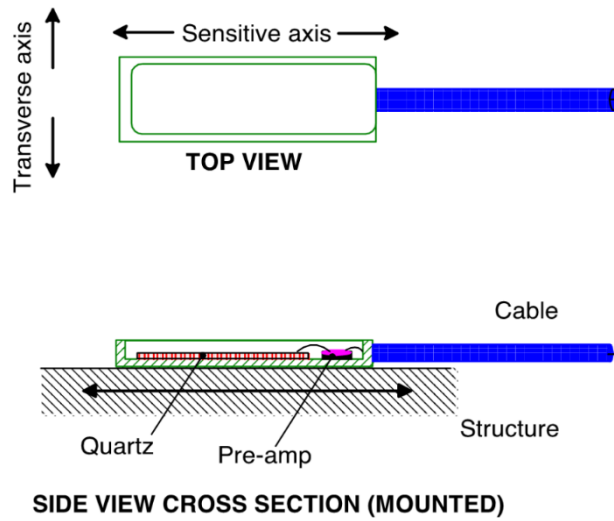


Figure 5: 740A02 strain sensor construction. Sensitive and transverse axis indicated in top view. Cross section shows mounting to structure

The sensor, as just mentioned, is mounted to the structure under test via an adhesive bond. For accurate measurements and good strain transfer to the sensor, the mounting surface must be clean and flat so the adhesive layer is thin and of high stiffness. The strain sensor's sensitivity is calibrated by using a steel cantilever beam. When the stiffness modulus of the structure under test is less than the modulus of steel, the actual sensitivity is less than the calibrated sensitivity.

The upper limit of the frequency response is determined either by cable drive considerations or by wavelength of dynamic strain. Long cables capacitively load the frequency output, and with long cables, measurement of high frequency may require the use of a higher current power supply. Measurements are accurate when the wavelength is large compared to the length of the sensor. The wavelength can be determined from the following formula [18]:

$$\lambda = c/f \quad (6)$$

where  $c$  is the speed of sound and  $f$  is the frequency. A good rule of thumb is that the wavelength can be determined from the following equation:

$$f_u = 0.1 \cdot c/L \quad (7)$$

where  $L$  is the length of the sensor.

Low inherent transverse sensitivity is one reason that a quartz sensing element, rather than piezoceramic, is used in the 740A02 strain sensor. Based on the cut of quartz, the inherent transverse sensitivity of the 740A02 sensor is equal to -1.9%. This means that if the sensitivity is 50 mV/ $\mu\epsilon$  along the sensing axis, the sensitivity transverse to this axis will be -0.95 mV/ $\mu\epsilon$ .

By design, the sensitivity to in-plane shear strain is zero. The following acceptance test, using the calibration beam shown in Figures 6 and 7, can determine the transverse sensitivity to an accuracy of 5% (a more accurate method is being developed that will determine transverse strain with an uncertainty of  $\pm 0.5\%$ ).

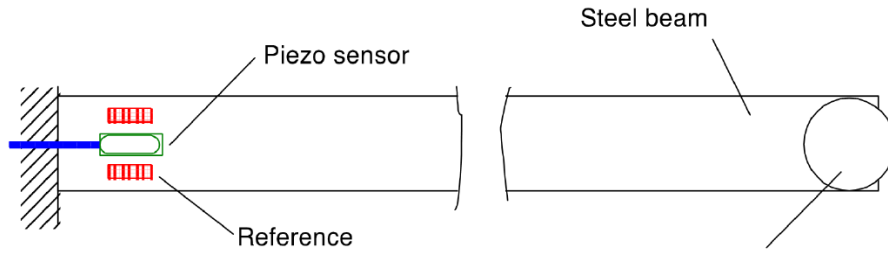


Figure 6. Cantilever beam for determination of sensitivity. (26 x 2 x 0.25 inches steel beam)

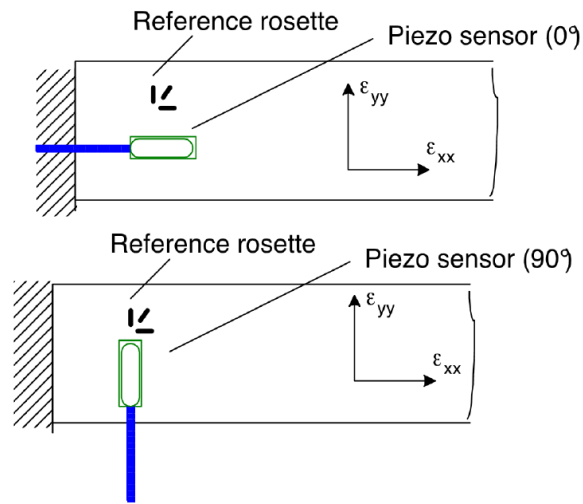


Figure 7. Determination of transverse sensitivity. Piezo sensor mounted at 0 and 90 degrees

The piezoelectric sensor is mounted at 0 and 90 degrees and the output is recorded. The measured strain field is also recorded:

$$\varepsilon = \begin{bmatrix} \varepsilon_{xx} & \varepsilon_{xy} \\ \varepsilon_{yx} & \varepsilon_{yy} \end{bmatrix} = \begin{bmatrix} \varepsilon_{xx} & 0 \\ 0 & \varepsilon_{yy} \end{bmatrix} = \begin{bmatrix} \varepsilon_{xx} & 0 \\ 0 & -\mu\varepsilon_{xx} \end{bmatrix}$$

(8)

As expected, the measured in-plane shear is equal to zero and  $\varepsilon_{yy}$  arises because of Poisson's effect. (The cantilever beam experiences uniaxial stress, but biaxial strain!) The output voltage is related to the strain field through:

$$V_0^0 = S\varepsilon_{xx}^0 + S_t\varepsilon_{xx}^0 \quad (9)$$

$$V_0^{90} = S_t\varepsilon_{xx}^{90} + S\varepsilon_{yy}^{90} \quad (10)$$

The superscripts 0 and 90 indicate measurements at  $0^\circ$  and  $90^\circ$  respectively. The above equations can be solved for the main axis and transverse sensitivities,  $S$  and  $S_t$ .

Below, we will describe a couple of application cases involving the use of the reusable dynamic strain sensor.



## 6 Reusable dynamic strain sensor in civil structure application

An example of an operational modal analysis test is briefly reported here regarding one experiment among many using the ICP reusable strain sensor in question for a civil structure.

In this case, an ongoing construction site has characteristics of dustiness and temperature changes such as would invalidate the use of traditional sensors, especially traditional foil strain gauges.

A normal process causes intermittent dynamic loading of building structural steel members [19]. The goal is to determine the force amplitude transmitted to the foundation and assess if bending exists in the columns. Given that this is dynamic loading of thick steel members, either foil or piezoelectric gauges can be used. As seen in Figure 8, the level of airborne contamination makes it virtually impossible to install foil gauges with any degree of confidence. Therefore, piezoelectric gauges have a clear advantage. Additionally, since several locations are to be monitored, installation of piezoelectric gauges provides substantial time savings over foil gauges. Figure 8 shows one side of an instrumented column. Two piezoelectric gauges were mounted to each column, one on each flange along the web centerline. Use of gauges mounted on opposite flanges allows for determining both axial and bending loads.

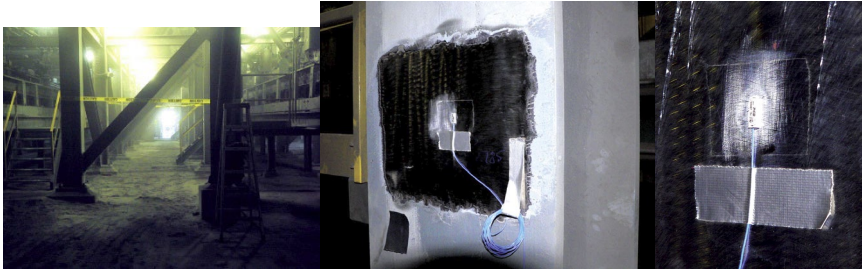


Figure 8. Test environment, columns to be instrumented and piezoelectric gauge mounted to building column flange at web centerline

Figure 8 also shows a closer view of a mounted piezoelectric gauge. Figure 9 shows time history strain data measured on the flanges of one of the columns.

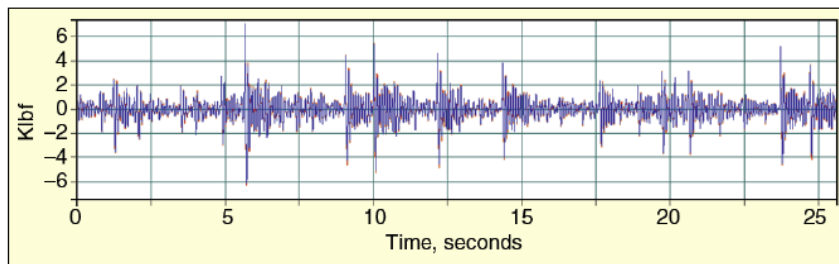


Figure 9. Time history strain data measured on the flanges of one of the columns

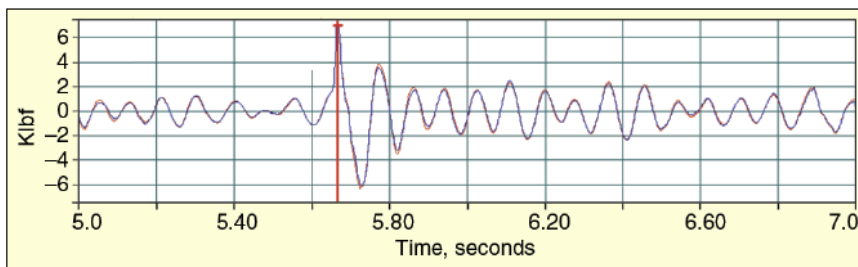


Figure 10. Strain time history at flanges of column showing pure axial loading

Figure 10 expands the data around 5.8 seconds to better show the waveforms. This figure clearly demonstrates that the column experiences pure axial loading (red and blue curves are identical in amplitude). Column geometry and material properties are used with gauge sensitivity to calculate calibration values that produce engineering units in force pounds. These data also demonstrate a sign convention difference between piezoelectric and foil gauges. When a compressive load is applied to a foil gauge, a negative voltage is output from the transducer signal conditioners. Conversely, a positive voltage is output when a compressive load is applied to the piezoelectric gauge. Figures 11 and 12 show data for a column that has a combination of axial loading (red and blue curves are in-phase) plus bending (red and blue curves have different amplitude).

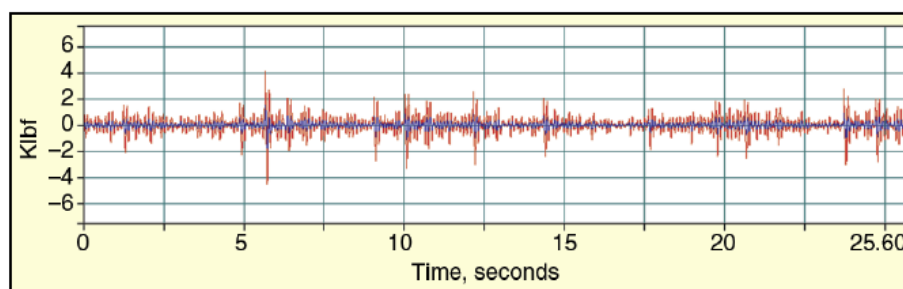


Figure 11. Strain time history at flanges of column

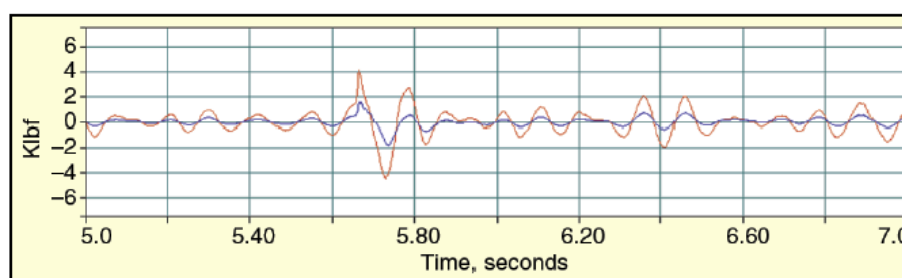


Figure 12. Strain time history at flanges of column showing axial plus bending

Piezoelectric strain gauges were evaluated under hostile conditions that would render foil gauge installation futile. In the above case history, piezoelectric gauges were found to have distinct advantages of being quickly mounted in dirty environments. Installation of piezoelectric gauges was achieved without shutting down process operation. It would have been virtually impossible to install foil gauges in such a dirty place, especially considering that this strain gauge is compensated in acceleration, a very useful characteristic on civil construction sites. Furthermore, because of the internal quartz crystal, it is also insensitive to temperature changes, therefore its sensitivity remains consistent with the specifications in case of temperature changes for field installations. Piezoelectric gauges are suitable for a high percentage of engineering studies, vibration troubleshooting projects, and failure investigations. The final benefit is that the gauges are reusable, allowing for greatly expanded studies with minimal setup time.

## 7 Strain Modal Analysis Applied to Ground Vibration Testing of an F-16

The ground vibration test campaign was carried out using the traditional instrumentation plus the piezo strain sensors described in the previous section. This test campaign was part of the LMS (now Siemens) GVT Master Class [17, 18]. In total, 136 measurements were obtained from the instrumentation in the whole aircraft. Of these, 17 were strain sensors placed on the left wing, 2 were force cells, and the rest were from accelerometers as shown in Figure 13. On the left wing, 8 triaxial accelerometers were placed in collocation with the strain sensors.

An LMS SCADAS Lab and a SCADAS mobile were used for the data acquisition, and 2 shakers were used to excite the structure, near the tip of each wing. To obtain a boundary condition close to free-free, the landing gear tires were slightly deflated, to decrease their stiffness. The left wing was instrumented with the strain sensors, as shown in Figure 14 with a close-up on one of the (nearly) collocated sensor pairs.



Figure 13. F-16 test set-up



(a) F-16 Left wing set-up

(b) F-16 left wing -  
collocated strain sensor  
and accelerometer

Figure 14. F-16 test set-up and close-up on left wing with strain sensor and accelerometer-collocated strain sensor and accelerometer

The aircraft was excited using the standard types of excitation signals, such as burst random, pseudo random, sine sweep and stepped sine. These different types of signals can be used to achieve different identification objectives, for example, to identify non-linearities. In the case of the tests using the strain sensors, the main objective was to visualize the strain and displacement modes on the left wing, and better understand their behavior. For this purpose, the burst random excitation was adequate and could provide good input for the modal identification procedure. As just mentioned, multiple excitation techniques have been used: burst random, pseudo random, sine sweep and stepped sine. Pseudo random has a better SNR than burst random, but we have chosen it to illustrate the performance of the ICP strain sensors by using burst random because it is still often used in the industry, and we are also able to demonstrate that even with non-optimal SNR, the ICP sensors work very well.

The full bandwidth of the excitation signal ranged from 1 to 64Hz, but a smaller range was used for the identification—there were enough modes present from 4.5 to 15 Hz. Figure 15 shows the strain frequency response function (SFRF) and the frequency response function (FRF), as well as their respective coherence function, from an arbitrary point on the left wing where a collocated pair of sensors was present.

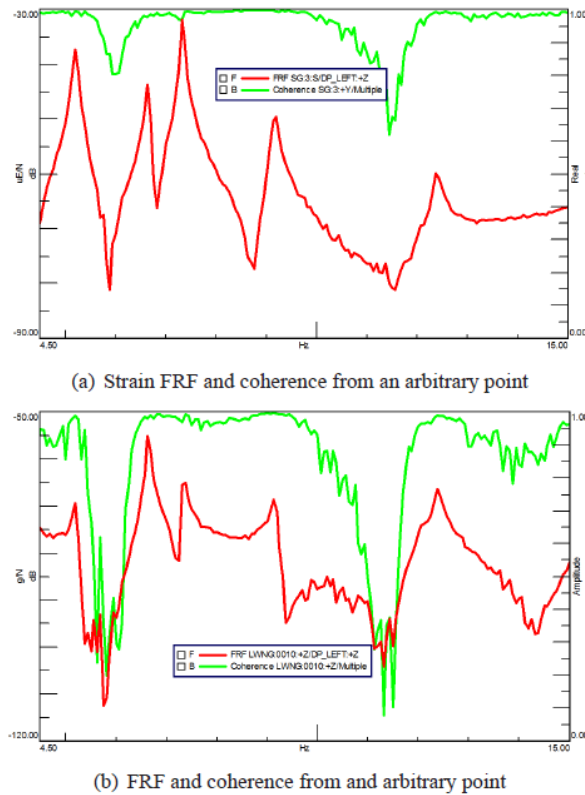


Figure 15. SFRF, FRF, and coherence functions from a collocated sensor pair on the left wing

A noticeable characteristic of the piezo strain sensors is their signal-to-noise ratio. As seen in Figure 15(a), the quality of the SFRF is very good, and the signal appears less noisy than the accelerometer.

The next step was to carry out the modal identification procedure. The vibration modes were estimated using the PolyMAX polyreference least-squares complex frequency-domain method [22]. By simultaneously using the accelerometers and strain sensors in the identification procedure, it was possible to visualize both displacement and strain components of the mode, where the strain could be displayed with coloring, while the displacement mode was represented by the actual displacement on the geometry. Both strain and acceleration sensors are indeed used together in the identification. Theoretically, it is possible to have mixed-units FRFs which is also implemented as such in Simcenter Testlab. The main advantages are that we only have to do the identification once and thus a consistent set of modes is obtained. If we were to analyze strains and accelerations separately, theoretically the same poles should still be found, but the risk of inconsistencies in the pole selection increases.

Another advantage is that strains and accelerations give complementary information: at clamps (e.g. wing-fuselage connection), strains are high and accelerations low; at free ends (e.g. wing tips), strains are low and accelerations high. The first mode of the aircraft is a symmetric wing bending mode, followed by an anti-symmetric torsional mode of the wings, then a symmetric torsional mode, and finally an anti-symmetric bending of the wings. The last two identified modes are the in-plane mode on the wings and the second symmetric bending of the wing. All these modes are shown in Figures 16 through 18.

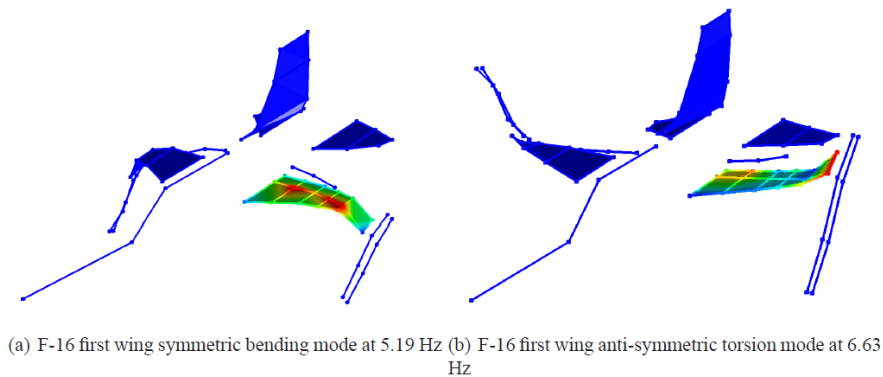


Figure 16. F-16 displacement and strain modes on left wing.

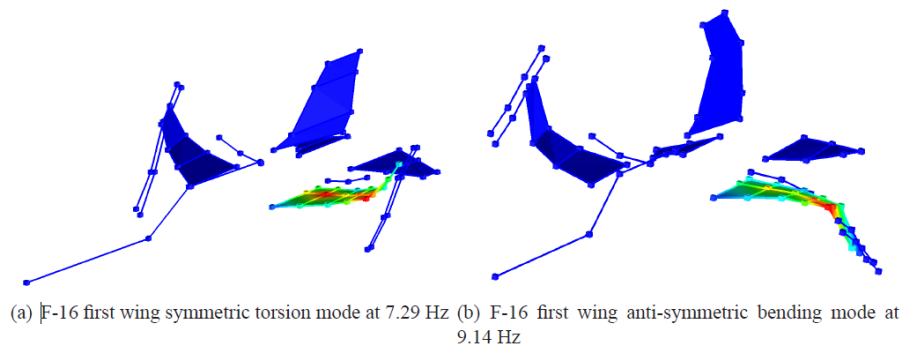


Figure 17. F-16 displacement and strain modes on left wing.

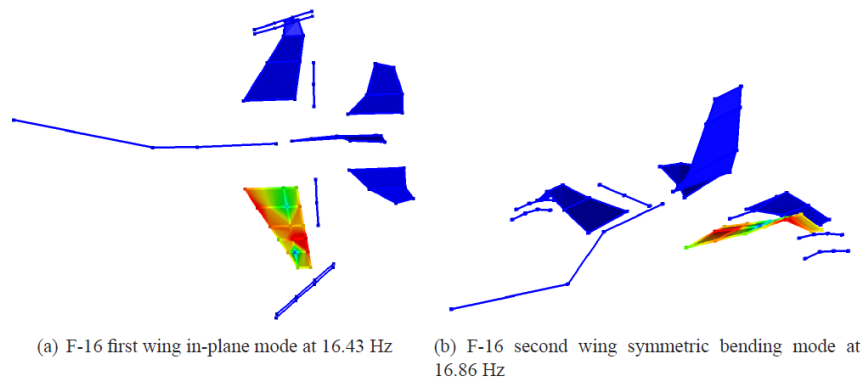


Figure 18. F-16 displacement and strain modes on left wing.

The modes show that the strain pattern in the wing cannot always be directly inferred or understood from the displacement modes. In the first case shown in Figure 17(a), for the wing bending, there is a high concentration of strain in the middle of the wing, possibly because of the complex internal structure of the wing. In the second case shown in Figure 17(b), the strain measurements clearly help in visualizing the high amount of stress incurred on the tip of the wing, where the attachment to the bomb is located. For the in-plane mode of the wings shown in Figure 18(a), it is clear that there is strain on the leading and trailing edges of the wing, meaning that the strain sensors are effective in capturing strain not only in the bending direction.

## 8 Conclusions

In this paper, the use of dynamic strain sensors for both a civil structure application and the ground vibration testing (GVT) of an F-16 aircraft were shown. Initially, the theory for strain modal analysis was presented, highlighting the differences and similarities between the accelerometer-based and strain gauge-based modal analysis. Then, the characteristics of the dynamic strain sensors were presented, also providing information on their sensitivity and how they are calibrated. A more extensive description was given of the response sensors, accelerometers, and strain sensors, which play a main role as response sensors for OMA tests and were used in the illustrated case studies. An example of a civil structure application was summarized, showing the benefits of the above-described reusable strain sensor in a harsh environment.

The set-up for the GVT was introduced, along with the measurement locations for the accelerometers and strain sensors used. The initial strain FRFs showed very good quality with respect to the signal-to-noise ratio, and the modal identification was carried out using those measurements. As a result, mixed strain and displacement mode shapes were shown, making it possible to see the strain pattern on the left wing of the aircraft with respect to its motion.

With the results, it is possible to conclude that the strain measurements can be used both in OMA for civil structure applications and also in a GVT campaign, and that the additional information provided by them is useful for further interpretation of the mode shapes, especially with complex structures.

## Acknowledgments

I thank the engineers of Siemens (formerly LMS), Bart Peeters, and the other authors with whom I wrote the paper [1] on which the main case study used in this work is based.

## References

- [1] F.L.M. Santos, B. Peeters, J. DeBille, C. Salzano, L.C.S. Góes, W. Desmet. The Use of Dynamic Strain Sensors and Measurements on the Ground Vibration Testing of an F-16 Aircraft. In *Proceedings of IFASD 2015 International Forum on Aeroelasticity and Structural Dynamics*, 2015.
- [2] R.J. Dieckelman, A.J. Hauenstein, and R.P. Ritzel. The ground vibration test - a boeing ids perspective. In *Proceedings of IMAC-XXIII International Modal Analysis Conference*, 2005.
- [3] Dennis Gge, Marc Bswald, Ulrich Fflekrug, and Pascal Lubrina. Ground vibration testing of large aircraft state-of-the-art and future perspectives. 2007.
- [4] C.R. Pickrel, G.C. Foss, A.W. Phillips, R.J. Allemang, and D.L. Brown. New concepts gvt. In *IMAC XXIV International Modal Analysis Conference*, 2006.
- [5] O. Bernasconi and D. J. Ewins. Application of strain modal testing to real structures. In *Proceedings of the 7th International Modal Analysis Conference*, volume 2, pages 1453–1464, 1989.
- [6] L. M. Vari and P. S. Heyns. Using strain modal testing. In *Proceedings of the 12th International Conference on Modal Analysis*, volume 2251, page 1264, 1994.
- [7] M. Luczak, A. Vecchio, B. Peeters, L. Gielen, and H. Van der Auweraer. Uncertain parameter numerical model updating according to variable modal test data in application of large composite fuselage panel. *Shock and Vibration*, 17(4-5):445–459, 2010.
- [8] T. Kranjc, J. Slavic, and M. Boltezar. The mass normalization of the displacement and strain mode shapes in a strain experimental modal analysis using the mass-change strategy. *Journal of Sound and Vibration*, 332(26):6968–6981, 2013.
- [9] A.M. Calabro, C. Salzano. Take the strain: new technologies for dynamic strain measurement sensors. *Aerospace Testing International*, pages 128–129, October 2007.
- [10] A. C. Pisoni, C. Santolini, D. E Hauf, and S. Dubowsky. Displacements in a vibrating body by strain gage measurements. In *Proceedings of the 13th International Conference on Modal Analysis*, 1995.
- [11] PCB Piezotronics Inc., Technical data from [www.pcb.com](http://www.pcb.com)

- [12] Simone Manzato, Fabio Santos, Bart Peeters, Bruce LeBlanc, and Jonathan R White. Combined accelerometers-strain gauges operational modal analysis and application to wind turbine data.
- [13] Matthew Whelan and Kerop Janoyan. Design of a robust, high-rate wireless sensor network for static and dynamic structural monitoring. *Journal of Intelligent Material Systems and Structures*, 2008.
- [14] H Xia, Guido De Roeck, N Zhang, and Johan Maeck. Experimental analysis of a highspeed railway bridge under thalys trains. *Journal of Sound and Vibration*, 268(1):103–113, 2003.
- [15] Fabio Luis Marques dos Santos, Bart Peeters, Raphael Van der Vorst, Wim Desmet, Luiz Carlos, and Sandoval Goes. The use of strain and mixed strain/acceleration measurements for modal analysis.
- [16] H Lie and KE Kaasen. Modal analysis of measurements from a large-scale model test of a riser in linearly sheared flow. *Journal of fluids and structures*, 22(4):557–575, 2006.
- [17] AD Trim, H Braaten, H Lie, and MA Tognarelli. Experimental investigation of vortex induced vibration of long marine risers. *Journal of fluids and structures*, 21(3):335–361, 2005.
- [18] Jeffrey J. Dosch. Piezoelectric strain sensor. In *Proceedings of IMAC XVII International Modal Analysis Conference*, 1999.
- [19] Chris D. Powell. Vibration Troubleshooting with Piezoelectric Strain Gages. *Sound and Vibration Magazine*, pages 20-23, September 2007.
- [20] Jenny Lau, Bart Peeters, Jan DeBille, Quentin Guzek, Willam Flynn, Donald S Lange, and Timo Kahlmann. Ground vibration testing master class: modern testing and analysis concepts applied to an f-16 aircraft. In *Advanced Aerospace Applications, Volume 1*, pages 221–228. Springer, 2011.
- [21] Bart Peeters, Alex Carrella, Jenny Lau, Mauro Gatto, and Giuliano Coppotelli. Advanced shaker excitation signals for aerospace testing. In *Advanced Aerospace Applications, Volume 1*, pages 229–241. Springer, 2011.
- [22] B. Peeters, H. Van der Auweraer, P. Guillaume, and J. Leuridan. The polymax frequency domain method: a new standard for modal parameter estimation? *Shock and Vibration*, 11:395–409, 2004.



**3425 Walden Avenue, Depew, NY 14043 USA**

pcb.com | info@pcb.com | 800 828 8840 | +1 716 684 0001

© 2024 PCB Piezotronics - all rights reserved. PCB Piezotronics is a wholly-owned subsidiary of Amphenol Corporation. Endevo is an assumed name of PCB Piezotronics of North Carolina, Inc., which is a wholly-owned subsidiary of PCB Piezotronics, Inc. Accumetrics, Inc. and The Modal Shop, Inc. are wholly-owned subsidiaries of PCB Piezotronics, Inc. IMI Sensors and Larson Davis are Divisions of PCB Piezotronics, Inc. Except for any third party marks for which attribution is provided herein, the company names and product names used in this document may be the registered trademarks or unregistered trademarks of PCB Piezotronics, Inc., PCB Piezotronics of North Carolina, Inc. (d/b/a Endevo), The Modal Shop, Inc. or Accumetrics, Inc. Detailed trademark ownership information is available at [www.pcb.com/trademarkownership](http://www.pcb.com/trademarkownership).

WPL\_98\_0924